

LASER INTERFEROMETER GRAVITATIONAL WAVE OBSERVATORY  
- LIGO -  
CALIFORNIA INSTITUTE OF TECHNOLOGY  
MASSACHUSETTS INSTITUTE OF TECHNOLOGY

Technical Note	LIGO-T2400157-v1	07/14/2024
<b>2024 LIGO SURF Interim Report 1: Frequency Locking a Laser to <math>^{87}\text{Rb}</math></b>		
Briana A. Chen		

California Institute of Technology  
LIGO Project, MS 18-34  
Pasadena, CA 91125  
Phone (626) 395-2129  
Fax (626) 304-9834  
E-mail: info@ligo.caltech.edu

Massachusetts Institute of Technology  
LIGO Project, Room NW17-161  
Cambridge, MA 02139  
Phone (617) 253-4824  
Fax (617) 253-7014  
E-mail: info@ligo.mit.edu

LIGO Hanford Observatory  
Route 10, Mile Marker 2  
Richland, WA 99352  
Phone (509) 372-8106  
Fax (509) 372-8137  
E-mail: info@ligo.caltech.edu

LIGO Livingston Observatory  
19100 LIGO Lane  
Livingston, LA 70754  
Phone (225) 686-3100  
Fax (225) 686-7189  
E-mail: info@ligo.caltech.edu

# 1 Introduction

The GQuEST (Gravity from the Quantum Entanglement of Space-Time) experiment aims to detect a quantum gravity signal by measuring phase differences of photons due to fluctuations in spacetime. If successful, this would be an exciting step in developing the theory of quantum gravity.

GQuEST has the same fundamental setup as LIGO (Laser Interferometric Gravitational-Wave Observatory). Light travels down and back the two arms of a Michelson interferometer and recombines. The phase difference between the two light beams is measured and analyzed in search of a statistically significant signal. The presence of any additional motion of the mirrors (in LIGO for example, a gravitational wave with frequency  $\epsilon$ ) will modulate the carrier (i.e. laser) frequency  $\nu_c$ , producing components of light at sideband frequencies  $\nu_c \pm \epsilon$  [1]. In LIGO, a DC readout method extracts the interference between these sidebands and the original laser frequency. In GQuEST, photon counting will be used to extract the photons of a specified frequency from the interferometer setup. The photons of interest will then pass through the optical filters, which can be a series of cavities. These cavities have the property that light can only transmit through if it is on resonance, or of a certain frequency  $\nu$ .

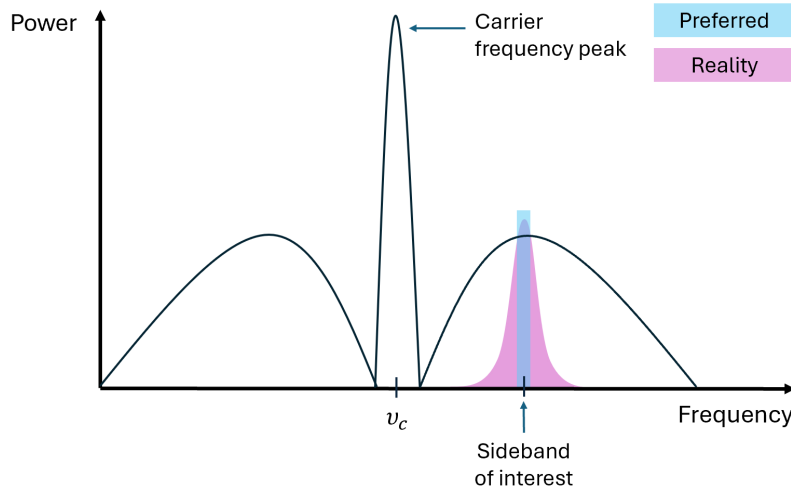


Figure 1: Preferred and actual behavior of optical filters. Due to noise, the laser will sometimes drift in frequency. The power spectrum of the recombined light from the interferometer will display a single prominent peak around the carrier frequency along with a smooth curve on either side of the peak that represents the sidebands formed from a stochastic quantum gravity signal. Noise is not shown on top of this power spectrum. The optical filter should solely isolate the intensity from the frequency of interest but in reality, will pick up signals of other frequencies.

Ideally, you want the transmitted light to behave like a unit impulse, where only light of the frequency  $\nu$  can pass. However, in reality, the transmitted light from the optical cavity will have a Lorentzian spectrum (see Figure 4 for the transmission shape). One can obtain a sharper peak by placing  $N$  cavities one after another such that the Lorentzian shape is raised to the  $N$ th power, narrowing the linewidth and improving signal-to-noise. An even better

option would be to use atomic cells instead of optical cavities as the resulting transmission lineshape will take on other forms like Gaussian, which could significantly improve the signal-to-noise ratio.

Designing better optical filters is necessary to amplify the signal-to-noise ratio at the sideband of interest as well as suppress the carrier. They must be tested and adjusted to minimize leakage outside their intended frequency range. The goal of this project is thus to produce a laser locked to a stable frequency suitable for future testing of these optical filters in the GQuEST experiment. However, the premise of laser locking has applications even in LIGO to reduce the number of free variables in the system.

### 1.1 How does a laser's frequency drift?

Lasers work by exciting electrons in some medium that amplifies light through population inversion. This inversion produces a higher population of atoms in the excited state. Undergoing the process of stimulated emission, the atoms drop down in energy level and release a photon. This photon is reflected back into the medium to produce more photons of the same energy in an optical cavity. The greater amount of reflections in unison produces more photons and ultimately, the energy of the photons enables them to pass through the mirror, producing the laser beam [2].

The gain medium will have different properties with shifts in temperature or the laser's mechanical properties. For example, changes in the medium's temperature shift the laser's gain curve, changing the laser output power and emission properties [3]. Other effects on laser emission include pressure changes, environmental effects, age, and electromagnetic fields, all of which contribute to frequency drifting [3].

### 1.2 Pound Drever-Hall (PDH) Locking

The basic process behind locking a laser's frequency is to measure the laser's frequency, determine how far away this frequency is from a cavity's resonant frequency, and then send the error back into the laser input to tune the laser. Figure 2 depicts the experimental feedback cycle of Pound Drever-Hall (PDH) locking, which has been a standard method of laser locking with an optical cavity.

To measure the frequency difference, the PDH technique uses a Fabry-Perot cavity, which has the important property that the total reflected and transmitted intensity is dependent on the frequency of light sent into the cavity [4]. The cavity consists of two partially transmissive and reflective surfaces that cause higher-order reflections and transmissions.

Assuming the surfaces have uniform reflection and transmission coefficients, the material between the two surfaces has a higher refractive index than those outside, and the beam

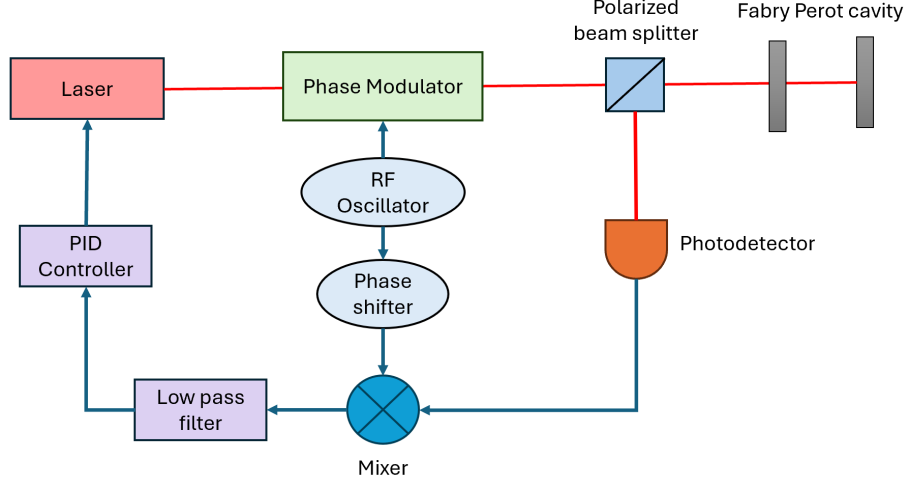


Figure 2: Basic schematic of PDH locking feedback loop [4].

enters with normal incidence, the electric field of the transmitted light is given by:

$$E_t = \frac{E_o t^2}{1 - |r|^2 e^{i\Delta}}$$

where we define  $\Delta$  as the phase acquired by the light from one round trip in the cavity, i.e.  $\Delta = \frac{\omega}{\Delta f_{sr}}$  [5].

The transmitted intensity is thus:

$$I_t = |E_t|^2 = \frac{I_o T^2}{|1 - R e^{i\Delta}|^2} = \frac{I_o}{1 + F \sin^2(\Delta/2)}$$

where the coefficient of finesse, a property of the cavity, is  $F = \frac{4R}{(1-R)^2}$ .

The electric field of the reflected light is similarly given by

$$E_r = E_o r \frac{1 - e^{i\Delta}}{1 - R e^{i\Delta}}$$

with the intensity being:

$$I_r = |E_r|^2 = \frac{I_o F \sin^2(\Delta/2)}{1 + F \sin^2(\Delta/2)}$$

Plotting the intensities, we can see that if the laser's frequency is in perfect resonance with the Fabry-Perot cavity (i.e. the laser frequency is an integer multiple of the cavity's free spectral range), the reflected intensity will be 0 [4]. This corresponds to a phase difference between the primary and leakage-reflected beams of 180 degrees (Figure 3).

However, if there is a shift in wavelength, we will measure some nonzero reflected intensity. Because the intensity curve is symmetric about resonance, we must use the derivative of the reflected intensity with respect to frequency to determine if we are above or below the resonant frequency. This is done by measuring the phase difference between the primary and

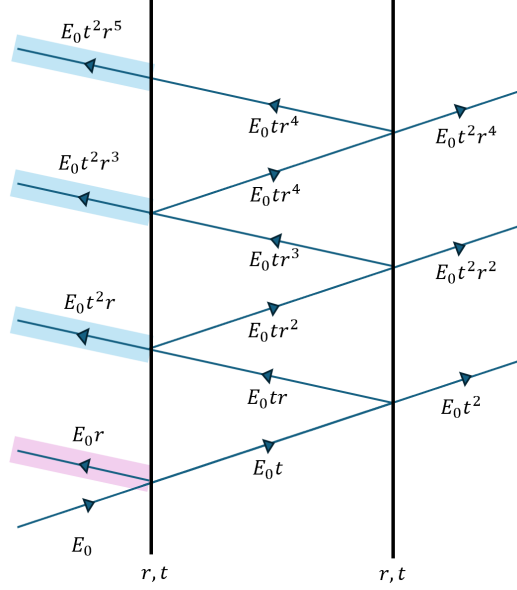


Figure 3: Simple Fabry-Perot cavity. Vertical black lines represent the cavity's surfaces. Dark blue lines represent the light's path and, assuming normal incidence, are drawn skewed to distinguish beams. Notice that the electric field of the reflected and transmitted beams can be written as a geometric series, which allows us to derive the subsequent equations. The primary reflected beam is highlighted in pink while the leakage reflected beams are highlighted in blue.

leakage reflected beams, which will constitute the error signal to be sent back to the laser [4].

To measure the phase difference between the reflected beam and leakage beams, we first modulate the incident beam by  $\beta \sin(\Omega t)$ , where  $\beta$  is the modulation depth,  $\omega$  is the carrier frequency, and  $\Omega$  is the phase modulation frequency. This gives us the following incident field entering the Fabry-Perot cavity [4]:

$$E_i = E_0 e^{i(\omega t + \beta \sin(\omega_m t))} \approx E_0 \left( e^{i\omega t} + \frac{\beta}{2} e^{i(\omega + \Omega)t} - \frac{\beta}{2} e^{i(\omega - \Omega)t} \right)$$

The first term describes the carrier (laser) frequency while the second and third term constitute the upper and lower sidebands, respectively. These sidebands (frequencies above or below the carrier frequency) are a byproduct of modulation.

Using what we know about Fabry Perot cavities, we can define the transfer function below to define the relationship between the input (incident beam) and output (reflected beam) from the cavity.

$$R(\omega) = \frac{E_r}{E_i} = r \left( \frac{e^{i\Delta} - 1}{1 - r^2 e^{i\Delta}} \right)$$

We apply this transfer function to the incident light  $E_i$  to obtain the electric field of the

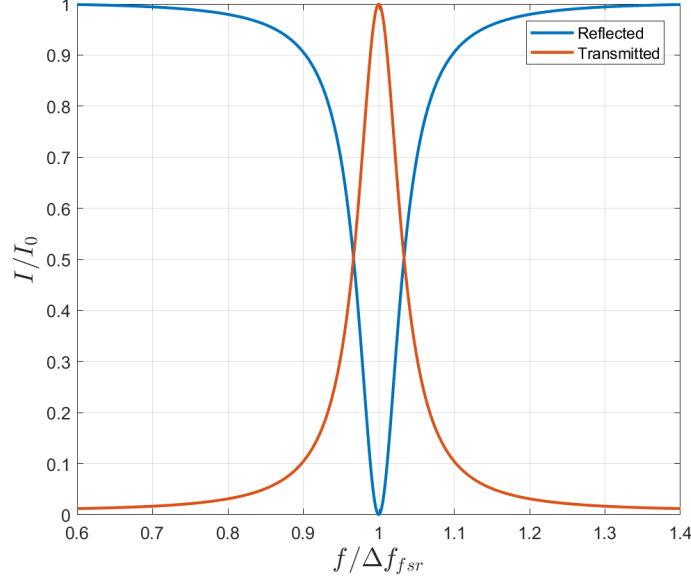


Figure 4: Fabry-Perot Intensity (transmitted/reflected beam). On resonance ( $\frac{f}{\Delta f_{fsr}} = 1$ ), the transmitted intensity is at a maximum while the reflected intensity is zero.

reflected light, whose magnitude squared yields the power of the reflected light,  $P_r$  [4]:

$$P_r = P_0 |R(\omega)|^2 + P_0 \frac{\beta^2}{4} (|R(\omega + \Omega)|^2 + |R(\omega - \Omega)|^2) + P_0 \beta [Re(\chi(\omega)) \cos(\Omega t) + Im(\chi(\omega)) \sin(\Omega t)] + (\text{terms in } 2\Omega)$$

where we define  $\chi(\omega) = R(\omega)R^*(\omega + \Omega) - R^*(\omega)R(\omega - \Omega)$  and  $P_0 = |E_0|^2$ . The terms involving  $\chi(\omega)$  represent the interference of the sidebands with the original laser beam (also referred to as the carrier beam), informing us about the carrier's phase.

The photodetector measures a voltage  $V_r$  that is proportional to the reflected power  $P_r$ . Subsequently, a mixer multiplies the measured voltage with the modulated signal  $\cos(\Omega t + \phi_m)$  to demodulate the beam and isolate the interference terms between the sidebands and carrier [4].

$$V_r' = V_r \cos(\Omega t + \phi_m) \propto P_r \cos(\Omega t + \phi_m) \propto P_0 [|R(\omega)|^2 + \frac{\beta^2}{4} (|R(\omega + \Omega)|^2 + |R(\omega - \Omega)|^2)] \cos(\Omega t + \phi_m) + P_0 \beta [Re(\chi(\omega)) \cos(\Omega t) + Im(\chi(\omega)) \sin(\Omega t)] \cos(\Omega t + \phi_m) + (\text{terms in } 2\Omega) \cos(\Omega t + \phi_m)$$

Setting the modulation phase  $\phi_m$  to 0 and selecting  $\Omega$  such that  $\chi(\omega)$  is purely real, we simplify this expression to:

$$V_r' \propto P_0 [|R(\omega)|^2 + \frac{\beta^2}{4} (|R(\omega + \Omega)|^2 + |R(\omega - \Omega)|^2)] \cos(\Omega t) + P_0 \frac{\beta}{2} \chi(\omega) \cos(2\Omega t) + P_0 \frac{\beta}{2} \chi(\omega) + (\text{terms in } 2\Omega) \cos(\Omega t)$$

The low pass filter isolates the constant term  $P_0 \frac{\beta}{2} \chi(\omega)$ , which informs us of the phase difference between the reflected and leakage beam and therefore the side of resonance we are on. Note that this will tell us whether we are on the positive or negative side as  $\chi(\omega)$  is an asymmetric function (Figure 5). This error will be fed back into the laser to tune the frequency, completing the feedback loop.

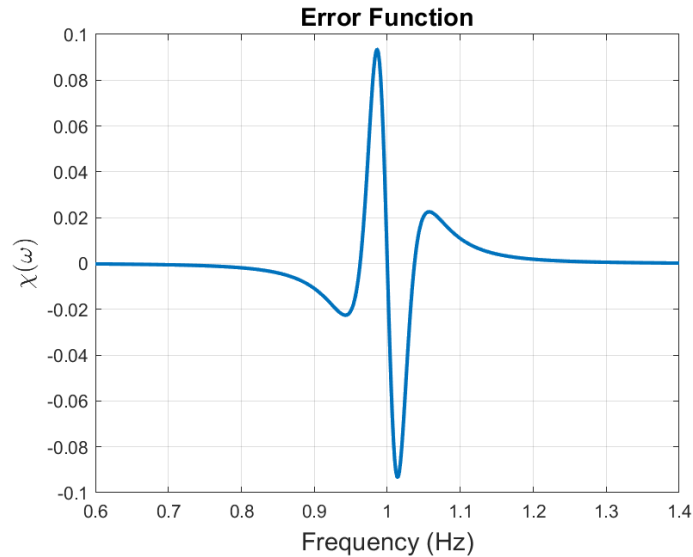


Figure 5: Real component of  $\chi(\omega)$  over frequency.

In summary, the PDH technique consists of the following steps:

1. Send modulated light into a Fabry-Perot cavity.
2. Measure the reflected intensity and demodulate the signal using a mixer.
3. Extract the error term using a low-pass filter, which informs us of which side of resonance the laser wavelength is on.
4. Send the error into the laser to tune it back onto the cavity resonant frequency (desired frequency).

This method allows us to correct the laser's frequency in real-time.

### 1.3 Locking a Laser to a Vapor Cell

While optical cavities yield good results for laser locking at a wide range of frequencies, they are a relative, not absolute, reference. The cavity itself must be stabilized very precisely against mechanical shifts, temperature changes, material expansions, and other environmental effects that could change the properties or distance between mirrors [3]. They must also be properly coupled to the laser's Gaussian modes. This begets another way of performing

laser locking, which is to use atomic transitions, an absolute reference. This method is not perfect as the atoms are affected by external electromagnetic fields and surrounding atoms, but overall, it permits more accurate locking due to the precise nature of atomic transitions [3].

First, consider a probe laser beam passing through a cloud of atoms. For simplicity, assume there are no external fields and there are only two energy levels (the ground and excited state). If the photons have resonant frequency  $\nu_0$ , the energy of photons in the laser beam is equal to the energy difference between the ground and excited state and thus the atom is energized from the ground to the excited state. If the atoms do not move and only absorb photons at resonant frequency  $\nu_0$ , absorption will only occur when the photons are all at resonant frequency  $\nu_0$ . Shockingly, atoms do move, so they will absorb radiation and become excited even if the photon is not at the resonant frequency due to Doppler shifting [6]. For example, if the atom is moving towards the laser, photons with frequencies below the resonant frequency will get absorbed because the atom "sees" the photons as being of higher frequency. Similarly, if the atom is moving away from the laser, photons with frequencies above the resonant frequency will get absorbed because the atom sees the photons as being of lower frequency. This is what gives the absorption curve its line shape and spread. This effect is known as inhomogeneous broadening, where absorption is dependent on the frequency of the incoming photon and the velocity of the atom. In homogeneous broadening, the decay of atoms from the excited to ground state produces the same fluctuations in frequency, such as stimulated emission. Typically, the resulting lineshape is a convolution of homogeneous and inhomogeneous broadening profiles (Lorentzian and Gaussian, respectively) [7]. Other broadening causes include collisions with other atoms, limitations of the laser bandwidth, and residual Doppler broadening if the pump-probe beams are not exactly antiparallel [3].

As with the PDH locking scheme, measuring the transmittance (in addition to measuring the derivative of the transmittance) will inform you of the amount of frequency detuning. However, in any locking scheme, a high-frequency discrimination (ability to distinguish between frequencies) is desirable [3]. To understand this, consider the graph in Figure 6a. If you have a narrower line width, you have stronger frequency discrimination because for a fixed change in frequency, the change in intensity is steeper than that of a wider line width. Thus, to sharpen the Doppler broadening effect and thereby increase frequency discrimination, a pump beam is sent into the vapor cell anti-parallel to the probe beam.

The pump probe works by first exciting atoms in the ground state with the probe beam. Then, the pump beam, which is at some potentially detuned frequency  $\nu$ , will excite the atoms traveling with a certain velocity due to the Doppler effect, carving a "hole" in the population of atoms in the ground state (known as Lamb dips, where the dips refer to the dip in the ground state population) [7]. The pump is typically stronger than the probe because its higher intensity will produce a stronger peak, although the exact width of the Lamb dips are dependent on factors like beam diameter, surrounding temperature, and external fields [7]. Lamb dips do not reduce transmission to zero because the pump only excites atoms of a certain velocity and not the entire population of atoms: the pump simply causes less of the probe beam to be absorbed.

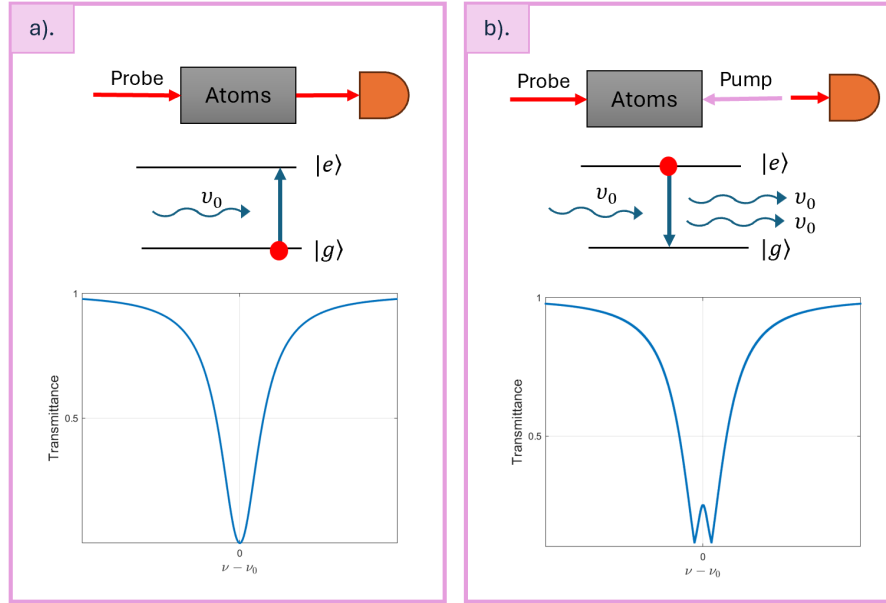


Figure 6: Graphs of the normalized transmittance as a function of laser frequency. a). Basic scheme of a laser passing through a vapor cell. If on resonance, the detector (orange) will measure no transmitted intensity because the energy provided by the incoming beam will be absorbed by all the atoms, energizing them to the first excited state. The transmittance shows a Doppler-broadened lineshape. b). The addition of a pump beam will cause stimulated emission at resonance, which knocks the atom down to ground state and produces two photons. This produces a small, narrow peak in transmittance symmetric around the atomic resonance frequency, which has a smaller linewidth than the overarching curve in (a).

The pump and probe are antiparallel to take advantage of this Doppler effect as off-resonance, the pump and probe beams excite different populations of atoms (traveling at different velocities in opposite directions) and thus act independently of each other. The probe will then primarily experience absorption [7]. However, if the probe and pump are near resonance, both beams will interact with atoms at velocity  $\vec{0}$ . As a result, those atoms will be excited by either the pump or probe beam. If the atom is excited by the pump, the atom is rendered "transparent" to the probe, which will enable it to transmit through the medium. As a result, we will achieve a peak in transmittance when both beams are on resonant frequency [7].

Another way of thinking about this is that when the probe beam passes through, stimulated emission occurs at resonance. If the pump has excited an atom to the excited state, the probe will knock the atom back down to the ground state, releasing one photon that travels coherently with the stimulating photon toward the detector. If off-resonance, the probe will experience more absorption from exciting an atom moving with certain velocity based on Doppler shift.

As evidenced in Figure 6, it is not possible to determine which side of resonance we are on due to the symmetry of transmittance peak around resonance. To find our error signal within this narrow range, we need to perform modulation and a similar process of error term extraction

as with PDH locking. If we modulate the probe beam, we obtain a carrier frequency  $\nu_c$  and sideband frequencies of  $\nu_c \pm \Omega$ . Upon passing through the nonlinear atomic medium, the previously unmodulated pump beam will become modulated, and the pump and probe will engage in four-wave mixing (FWM) [8]. FWM occurs when two or more beams indirectly interact within a nonlinear medium (in this case, the vapor cell), producing a new frequency due to scattering of incident photons. Typically, this occurs with three frequencies, which produces another frequency that is some sum/difference of the three initial frequencies. In this case, two pump photons (at some frequency  $\nu$ ) and a probe photon (at frequency  $\nu \pm \Omega$ ) interfere and produce a probe photon at sideband frequency  $\nu \mp \Omega$ . The interference between the probe and these sideband photons creates a modulation signal which is received by the photodetector [8].

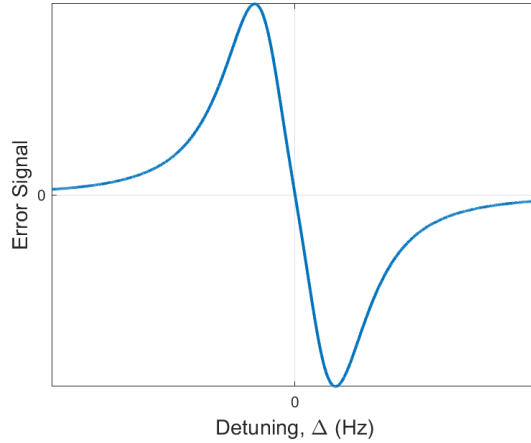


Figure 7: Error signal from modulation transfer spectroscopy method.

The signal is demodulated to generate an error signal as shown in Figure 7, which is a measure of the phase difference between the probe and its generated FWM sidebands (in PDH locking, this was the interference between the carrier and sidebands of the reflected beam). This signal is given by [8]:

$$S(\Omega) = \frac{C}{\sqrt{\Gamma^2 + \Omega^2}} J_0(\delta) J_1(\delta) ((L_{-1} - L_{-1/2} + L_{1/2} - L_1) \cos(\Omega t + \phi) + (D_1 - D_{1/2} - D_{-1/2} + D_{-1}) \sin(\Omega t + \phi))$$

where  $L_n = \frac{\Gamma^2}{\Gamma^2 + (\Delta - n\Omega)^2}$  and  $D_n = \frac{\Gamma(\Delta - n\Omega)}{\Gamma^2 + (\Delta - n\Omega)^2}$ , where  $\Gamma$  is the linewidth and  $\Delta$  is the amount of frequency detuning [8].

Similar to how we approached this in PDH locking, we can choose  $\Omega$  and  $\phi$  such that the signal is maximized and we are only left with the cosine or sine term of the error signal. The resulting error signal is asymmetric, as we saw for PDH, enabling us to determine which side of resonance we are on. This error can be fed back into the laser input to correct frequency drifts.

In general, the primary advantage of using this modulation method (also known as modulation transfer spectroscopy, or MTS) is that any absorption that remains after the probe

passes through the vapor cell does not affect the background, creating a stable baseline [3]. The signal is then relatively independent of polarization, temperature, and intensity in comparison to other methods [8]. Some limitations do apply and should be considered. For example, because modulation frequencies are smaller than natural linewidth, there is a bandwidth limit. MTS also only applies for atoms with cycling transitions, meaning that if the atom emits a photon going from excited to ground state, sending another photon in will energize it back to the same excited state. Finally, there is a limitation in the region of dithering because, as shown in Figure 6b, there is additional symmetry outside of the transmission peak. If the frequency is too far from resonance, the first order derivative will no longer satisfy the degrees of freedom in the graph.

## 2 Objective

The objective of this project is to lock a 1560 nm laser that has been frequency doubled to 780 nm to a vapor cell of rubidium atoms and verify the apparatus' ability to correct frequency drifts to a suitable sensitivity. We can quantify the success of the locking mechanism using the Allan variance, which measures the long-term variance in the laser frequency and will inform us about different noises in the system, which are distinguishable by the power laws they follow over time [3].

To successfully build the laser locking scheme, the following objectives must be obtained:

- The laser beam entering the system has a wavelength equivalent to the 780 nm closed transition in  $^{87}\text{Rb}$  energy levels. This will require some nonlinear crystal to halve the initial laser's frequency.
- The vapor cell is filled with  $^{87}\text{Rb}$  and is at a uniform temperature without interference from electromagnetic fields. This will require heating control and possibly magnetic shielding.
- The photodetector response is calibrated to a stable reference source to measure the transmittance of the probe through the vapor cell.
- The parameters of the phase modulator and demodulation filtering/mixing system (including the oscillator phase and frequency) are tuned to maximize error signal and, consequently, frequency discrimination. This tuning will occur for different modulation frequencies to obtain the highest signal.
- A PID controller or custom controller is designed to relate the laser's response to the error signal, tuning the amplitude, frequency, and phase of various signals and filters to reduce noise.

### 3 Approach

To lock a laser to a vapor cell of rubidium atoms, we will build something similar to the schematic in Figure 8, which is reminiscent of PDH locking except a vapor cell is now being used.

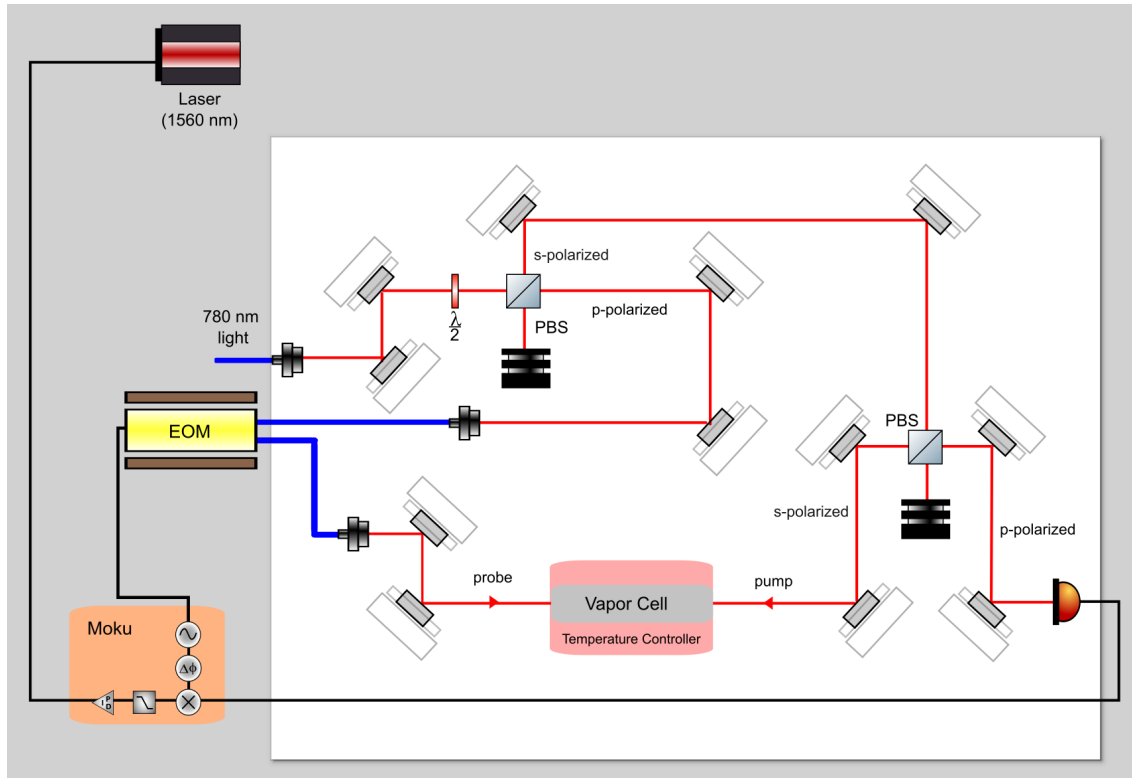


Figure 8: Schematic of laser locking to the rubidium vapor cell.

Rubidium atoms were chosen due to their heavier molecular mass, which narrows atomic Doppler widths. We will be locking a 1560 nm laser, but because the  $^{87}\text{Rb}$  atoms have limited atomic transitions corresponding to 780 nm, we will use a nonlinear crystal to double the original laser frequency via second harmonic generation.

After isolating the 780 nm light produced, the laser will be split into the probe and pump beam using a polarized beam-splitter. The two have the same frequency and detuning but the probe beam undergoes modulation prior to entering the vapor cell using an electro-optic modulator (EOM), producing the sidebands discussed in the previous section. After passing through the vapor cell, the intensity of the probe will be measured by a photodetector. The probe's transmittance allows us to determine the distance from resonance via the demodulation sequence, which produces an asymmetric error signal that is fed into the laser.

Faraday isolators are used to prevent unwanted reflected light from reentering the laser. We will additionally need to isolate contributions from the pump to the photodetector because it passes through the polarized beam splitter. Heating elements on the vapor cell will be used and controlled to maintain the vapor cell at a stable temperature to reduce temperature

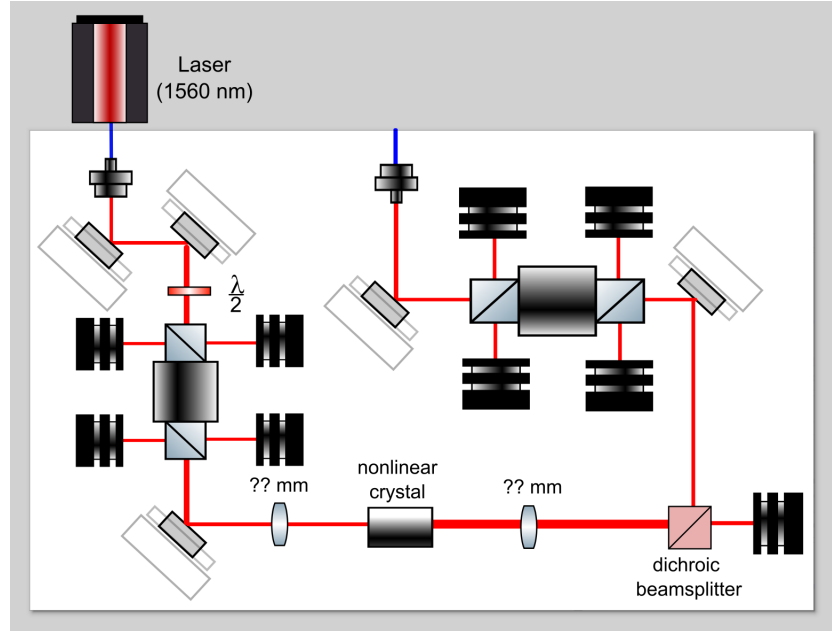


Figure 9: Second harmonic generation (SHG) schematic.

fluctuation effects. To maintain the width of the laser beam, especially as it passes through the vapor cell, additional optics will be used to collimate the beam or, at the very least, ensure the beam diameter is of consistent width as it reaches each element of the setup.

## 4 Progress

The setup has been split into two separate sleds for the SHG and the vapor cell portions respectively. This is for ease of transportation and swapping laser sources as a 780 nm laser can be easily connected to the vapor cell portion of the SHG. We have assembled most of the optics and placed them on two separate breadboards as indicated by the scaled schematics 89. We have also mechanically installed the vapor cell and its heater assembly. The items that remain to be set up are the 1560 nm laser, temperature controller for the vapor cell, and EOM.

We set up a 780 nm distributed Bragg reflector (DBR) laser to begin building the vapor cell setup, which can bypass the need for the SHG in case it does not work. The setup of the 780 nm laser includes a temperature and current controller, which together determine the power and wavelength of light from the laser. The appropriate limits have been placed on the current controller according to the laser diode specifications, but we still need to determine the proper current limits on the temperature controller.

For the second harmonic generation (SHG) setup, I learned to do mode matching using the JamMt software and a Nanoscan Photon beam profiler which, using the size of the beam (defined by the point on the beam spot at which the intensity has decayed by a factor of  $\frac{1}{e^2}$

) at different points along its path, can be used to calculate the location of the beam waist along the beam path. This will be useful for SHG as the beam profile prior to entering the nonlinear crystal and numerical apertures specified by the nonlinear crystal will determine the needed focal length of the lens such that the beam becomes narrow enough to enter the crystal.

We have also made a preliminary transmittance measurement verifying that the vapor cell works properly by sending the 780 nm laser beam through the cell, measuring the transmitted power with a photodetector, and scanning across the laser's temperature control such that we see the expected dip in transmittance. By changing the laser's temperature, we are changing the wavelength of light produced. At the dip in transmittance, the temperature corresponds to the 780 nm transition. The absorption dip, which is due to the atoms absorbing a photon that energizes it to the excited state, occurs as expected! 10

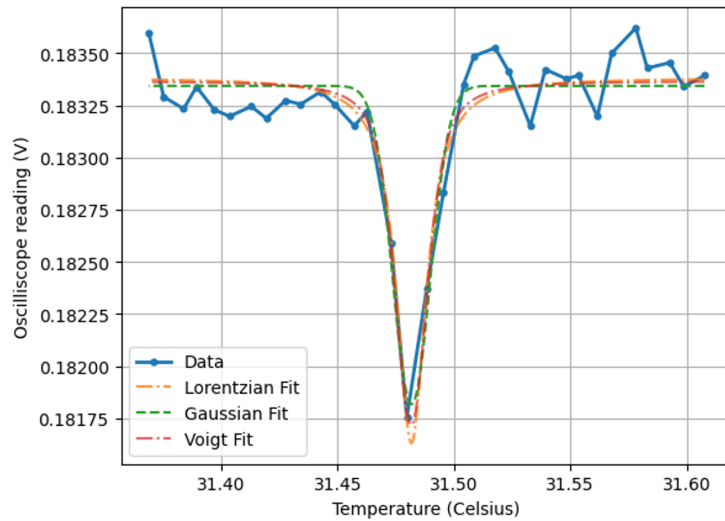


Figure 10: A measured absorption dip after scanning through the temperature range where the laser wavelength reaches 780.24 nm (around 30 to 33 °C). We would expect the absorption to have a Voigt profile since there is likely a combination of homogeneous and inhomogeneous broadening, meaning there is a convolution of the Lorentzian and Gaussian profile respectively that is known as a Voigt profile.

## 5 Challenges

A main challenge is ensuring the beam alignment matches the properties of the optics and behaves as expected. There have been a few challenges with this so far. For example, light initially did not seem to visibly transmit through a Faraday isolator, but this was due to a combination of misalignment and polarization. By adding a half waveplate, we solved the issue by properly aligning and maximizing power out of the isolator. Another example is when setting up the temperature controller on the 780 nm laser. We expected there to be a significant increase in temperature upon decreasing resistance based on the Steinhart-Hart

equation 5 given in the laser specifications, but we did not measure a significant increase using the surface temperature measurement tool. As a note, the Steinhart-Hart equation is given by:

$$\frac{1}{T} = A + B \ln R + C(\ln R)^3$$

where  $T$  is the thermistor temperature in Kelvins,  $R$  is the thermistor resistance in Ohms, and  $A$ ,  $B$ , and  $C$  are the Steinhart-Hart coefficients specific to the laser [9].

However, we concluded that this discrepancy was because the surface temperature was not reflective of the actual thermistor temperature inside the diode. By measuring the power of the laser at various current and temperature settings, we found agreement with the laser specifications and also verified that the laser diode was behaving as expected.

Another challenge has been fitting the schematics on a breadboard of fixed size. The SHG setup went through a few iterations to fit onto a smaller breadboard and may still require a bigger sled depending on the difficulty of alignment. However, determining the optimal configuration was a fun puzzle as there were different factors to consider such as back scattering from the beamsplitter or mirrors.

Another challenge has been being confident from the manuals that the settings of an equipment are correct. There is always potential to break something important by, for example, applying the incorrect current to a laser, so it is necessary to be thorough.

In terms of anticipated challenges, I foresee a lot of optical alignment in my future. One issue with this could be the offset in beam height from the SHG crystal, which will require proper steering before it is sent to the fiber coupling. Light through the vapor cell (of the probe and counterpropagating pump beam) will also need to be properly steered since the vapor cell produces a yaw offset.

Additionally, we will likely experience challenges with setting up the SHG as the waveguide must undergo phase matching to produce an appropriate intensity of 780 nm light. We will also implement a temperature controller on the vapor cell heating. The temperature will be selected to make the absorption dip as significant as possible. Maintaining a stable temperature will enable us to pack the states, ensuring as many atoms are in the  $5^2S_{1/2}$  level as possible (the level before the 780 nm transition) [10]. Tuning the waveguide and temperature control to achieve the optimal parameters will thus require trial and error. Finally, we still need to consider the specifics of how we will consistently quantify the drift of laser frequency, i.e. how we will compute the Allan variance or other metric from our data.

## Acknowledgements

Thanks and credit to Ian Macmillan for helpful discussion regarding this report.

## References

- <sup>1</sup>S. M. Vermeulen, T. Cullen, D. Grass, I. A. O. MacMillan, A. J. Ramirez, J. Wack, B. Korzh, V. S. Lee, K. M. Zurek, C. Stoughton, et al., “Photon counting interferometry to detect geotropic space-time fluctuations with gquest”, arXiv preprint arXiv:2404.07524 (2024).
- <sup>2</sup>*Nif’s guide to how lasers work*.
- <sup>3</sup>M. Mausezahl, M. F., and R. Low, “Tutorial on laser locking techniques and the manufacturing of vapor cells for spectroscopy”, *American Journal of Physics* **69**, 79–87 (2001).
- <sup>4</sup>E. D. Black, “An introduction to pound–drever–hall laser frequency stabilization”, *American Journal of Physics* **69**, 79–87 (2001).
- <sup>5</sup>J. Peatros and M. Ware, *Physics of light and optics* (Brigham Young University, 2023).
- <sup>6</sup>U. of Florida Department of Physics, *Saturated absorption spectroscopy*, 2020.
- <sup>7</sup>C. J. Foot, *Atomic physics* (Oxford University Press, 2005).
- <sup>8</sup>D. McCarron, S. King, and S. Cornish, “Modulation transfer spectroscopy in atomic rubidium”, *Measurement Science and Technology* **19**, 105601 (2008).
- <sup>9</sup>J. S. Steinhart and S. R. Hart, “Calibration curves for thermistors”, *Deep Sea Research and Oceanographic Abstracts* **15**, 497–503 (1968).
- <sup>10</sup>D. A. Steck, *Rubidium 87 d line data*, available online at <http://steck.us/alkalidata> (revision 2.1.4, 23 December 2010).